Ink Penetration of Uncoated Inkjet Paper and Impact on Printing Quality

Ren'ai Li,[a] Yan Zhang,[b,*] Yunfeng Cao,[a,*] and Zhulan Liu [a]

This study investigated ink penetration through imaging technology, first by gray and contour mapping and then calculating the ink penetration depth by programing. Next, a series of further analyses were carried out, including average ink permeability, ink distributions, and printability of different uncoated inkjet paper with different parameters. The impact on ink penetration of the microstructure and hydrophilicity of the uncoated paper was also studied. The experimental results indicated that paper specimens with sizing agent were resistant to the ink, resulting in a slow and shallow ink penetration. Paper containing filler had a more hydrophilic surface and porous structure, leading to a faster and deeper ink penetration. However, the calendering operation could make the paper structure more compact and reduce the porosity and penetration depth. When an appropriate combination of sizing agent, filler content, and the calendering process was utilized, a more stable hue could be produced with improvements in optical density, saturation, and color.

Keywords: Image technology; Ink penetration; Uncoated inkjet paper; Printing quality

*Contact information: a: Jiangsu Provincial Key Lab of Pulp and Paper Science and Technology, Nanjing Forestry University, Nanjing 210037, China; b: Henan University of Animal Husbandry and Economy, Zhengzhou 450046, China;*Corresponding author: yunfcao@163.com and yanzhang12@yeah.net*

INTRODUCTION

With the rapid development of the inkjet printing industry, there is a growing demand for uncoated inkjet paper. The requirements for uncoated paper should not be limited to the text and lines; it must be able to further satisfy the demands of simple color reproduction. Thus, there is a cost reduction space for substrates on the premise of meeting these primary needs. Uncoated inkjet paper with these advantages can fill the gap between fine coated paper and plain paper. Unfortunately, due to the lack of an "umbrella" of coating, the droplets emitted from the printer spread directly along the paper fibers and penetrate the bulk of the paper (Le 1998). This is a competitive process. If ink droplets spread across the surface faster than they penetrate, they could cause dot gain (Emmel and Hersch 2002), a longer drying time, and smearing. Conversely, if the ink droplets flowed into the paper fibers more, strike-through and poor optical density could result. Therefore, it becomes increasingly important to focus on the interaction between ink and the uncoated inkjet paper.

Current research projects on ink penetration employ various advanced equipment and technologies. Among them, microscope technology is receiving a lot of attention due to its accurate capture of paper information. Kishida *et al*. (2001) investigated the ink penetration of different coated paper cross-sections by scanning electron microscopy (SEM). Heard *et al.* (2004) studied the distribution of ink components in printed coated paper by combining focused ion beam (FIB) techniques with a transmission electron microscope (TEM), and found that paper with smoother surface and less porosity had a

lower ink demand. Ozaki *et al.* (2005) explored the penetration of the ink vehicle by staining it with a fluorescent dye and obtained a three-dimensional characterization using confocal laser scanning microscopy (CLSM). Considering the separation of some fluorescent dyes from the ink vehicle, Li and He (2011) employed UV-curing fluorescent rose ink as a substitute and investigated the penetration and distribution of ink pigments by CLSM. They also observed the microstructure of the paper surface by using atomic force microscopy (AFM) and showed that the large pores led to deeper penetration of ink pigments, and uniform ink absorption occurred when the pore distribution was uniform. Other novel techniques include using Cu as a tracer to study the penetration depth (Bülow *et al.* 2002; Varjos *et al.* 2004) and employing the chromatographic methods to study penetration and separation of cold ink resin and oils in uncoated paper (Mattila *et al.* 2003).

The modeling of ink penetration depth has also attracted a lot of attention in this field. Kubelka-Munk (K-M) theory (Kubelka and Munk 1931; Kubelka 1948) has been well received because of its simplicity. Li and Miklavcic (2005) explained some shortcomings of the K-M theory and revised it for more accurate applicability. Moreover, Li and Kruse (2000) proposed three kinds of penetration models depending on different penetration conditions of the paper. Utilizing a dynamic model, Daniel and Berg (2006) put forward a model based on energy arguments to study ink's spreading across, and penetration into, a thin, permeable print medium.

However, it has been found that most current studies still ignore information provided by microscopy and by computer technology, even though the combination of both can offer automatic, fast, and repeatable analysis. Therefore, this article proposes higher requirements for accurately exploring the ink penetration and distribution within the paper interior as well as its impact on print quality, so that further control over compositions or processing can be obtained. This will provide an improved understanding of ink-paper interactions.

EXPERIMENTAL

Materials

Five types of laboratory handsheets with varying parameters, each consisting of a mixture of 85% eucalyptus (35°SR) and 15% masson pine (35°SR) pulp, were used in this experiment. The grammage of these hand-sheets was 80 g/m^2. The sizing dosage (AKD), calcium carbonate dosage (PCC), and the calendering pressure were 0.1%, 25%, and 3 MPa, respectively. Two hand-sheets of each type were used as the substrates for repeated trials. The formulation of these uncoated papers is shown in Table 1.

Table 1. Formulation of Uncoated Handsheets

Handsheet	Parameters
Pap-1	$A_0B_0C_0$
Pap-2	$A_1B_0C_0$
Pap-3	$A_0B_1C_0$
Pap-4	$A_1B_1C_0$
Pap-5	$A_1B_1C_1$
*A, B, and C represented AKD, PCC, and calendering pressure. 1 = process employed, 0 = not.	

As shown in Fig. 1, the particle size distribution of PCC was measured with laser particle size analyzer from Dandong Bettersize Instruments, Ltd. The ash content and porosity of these hand-sheets in Table 2 were measured using a muffle furnace at 575 °C and mercury intrusion method (Autopore IV, USA), respectively.

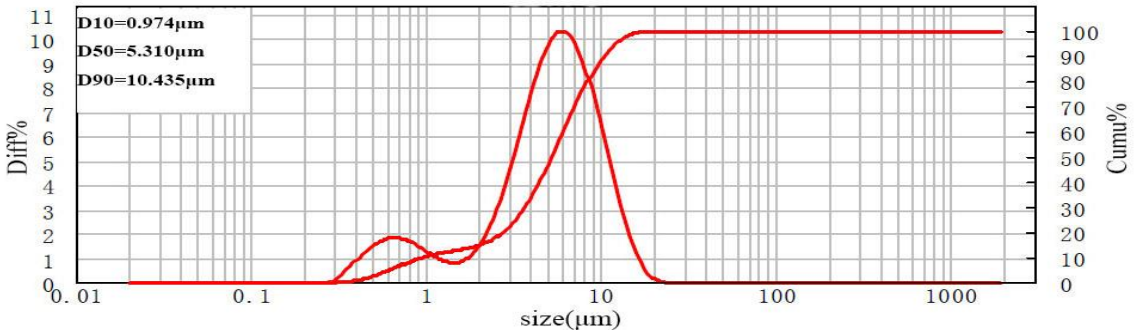

Fig. 1. Particle size distribution of PCC

Table 2. Properties of Uncoated Handsheets

Handsheet	Ash Content (%)	Porosity (%)
Pap-1	0.62	9.55
Pap-2	0.55	9.55
Pap-3	9.74	14.69
Pap-4	10.03	15.49
Pap-5	10.12	11.62

Methods

Printing

Standard image colors, including cyan, magenta, yellow, black, red, green, blue, and 3C (C+M+Y), depicted in Fig. 2, were printed by an Epson 7910 inkjet printer (Japan) with aqueous pigment-based inks at the temperature of 20 to 25 °C and under the relative humidity of 40% to 60%. The dot proportion was set at the range of 5% to 100%. The "Epson plain paper" setting was selected as the printing media.

Fig. 2. The standard image used for printing

Spectroscopic measurements

A GretaMacbeth SpectroEye spectrophotometer (Germany) with a D65 illuminant and UV-filter was used to measure the printing quality, including the optical solid density and the L^*, a^*, and b^* values of the color gradation from 5% to 100%. The measuring angle was constant at 2°, and the white area was defined as the unprinted paper.

Optical microscopy

In this work, the portions of the paper with solid cyan color were selected and its cross sections were observed by means of Confocal Laser Scanning Microscopy (Leica M205FA, Germany). The high-resolution images (1360×1024×3) of the ink penetration were photographed at a 101X magnification, in order to capture more ink pixels in the paper interior and then saved as ".tiff" format files.

Image processing

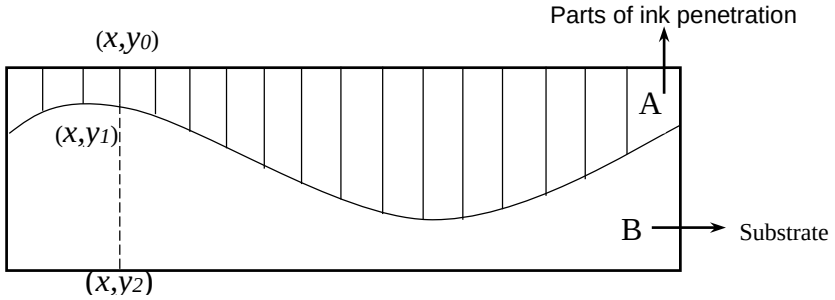

Fig. 3. The ink penetration depth

In fact, any color could be employed as the target sample as long as one is following the steps of image processing. Figure 3 is a schematic diagram of the cross section of a print. Due to the inhomogeneous structure of the paper, the depths of ink penetration varied significantly within each column. The image was shown in the form of a matrix (*m* rows, *n* columns), and the ink penetration depth in a column *x* was defined as (Eq. 1):

$$\Delta h(x) = y_1(x) - y_0(x), \quad x\epsilon[1, n\,] \tag{1}$$

In order to simplify the calculation, it was necessary only to determine the starting position y_0 and the ending position y_1. The subtraction of y_1 and y_0 yielded the ink penetration depth. The average ink penetration depths were thus calculated using Eq. 2.

$$\overline{h} = \frac{\sum_1^n \Delta h(x)}{n}, \quad x\epsilon[1, n\,] \tag{2}$$

$$\begin{bmatrix} 0 & 0 & \ldots & \ldots & 0 \\ 0 & 1 & 0 & 0 & 0 \\ \ldots & \ldots & 1 & 0 & 1 \\ \ldots & \ldots & \ldots & \ldots & \ldots \\ 1 & \ldots & \ldots & \ldots & 1 \end{bmatrix}$$

Fig. 4. The matrices of the ink penetration image (0, the pixel with ink; 1, the pixel without ink)

In order to clearly distinguish the boundary between the ink layer and the substrate, the gray and contour areas of the initial ink penetration image were mapped using Adobe Photoshop CS5 and MathWorks MATLAB 2012b software. The ink penetration portion of the image was easily identified from the rest of the image using Photoshop due to its high register in the red channel. Lastly, in order to determine the Δh across the columns (1 through *n*) of the image matrix, the ink layer image of binarization was read in the MATLAB software, as shown in Fig. 4.

RESULTS AND DISCUSSION

Image Extraction and Ink Penetration Depth Calculation

As shown in Fig. 5 and Table 3, the variance of Pap-1 was relatively small, and the contour mapping exhibited a uniform ink penetration around fibers. The average ink penetration depth in Pap-2 (with sizing) was smaller than Pap-1 and Pap-3, but the variance was higher than the other two samples, as would be expected given the hydrophobization of the fibers. At the same time, the distributions of the pigments in Pap-2 were less homogeneous, due to the more limited pathways for liquid absorption and possibly due to the inhomogeneous distribution of the sizing agent. The contour mapping of Pap-3 (with fillings) gave the lowest variance, which suggested the most even penetration distributions of all paper types.

Compared to Pap-4, ink penetration depth and variance in Pap-5 was greatly reduced after calendering; this was attributed to the more compact structure and lower porosity. Due to the sizing agent both existing in Pap-2 and Pap-4, the variances of ink penetration were larger than Pap-1 and Pap-3, indicating that sizing agent could cause a less even ink distribution.

In addition, the ink penetration depths and variances differed from sample to sample, indicating that the different parameters that distinguished the samples had an impact on ink penetration. Moreover, the analysis on the data of different samples calculated by the programing was able to compensate for the limitations of the subjectivity of the image comparisons (Li *et al*. 2005).

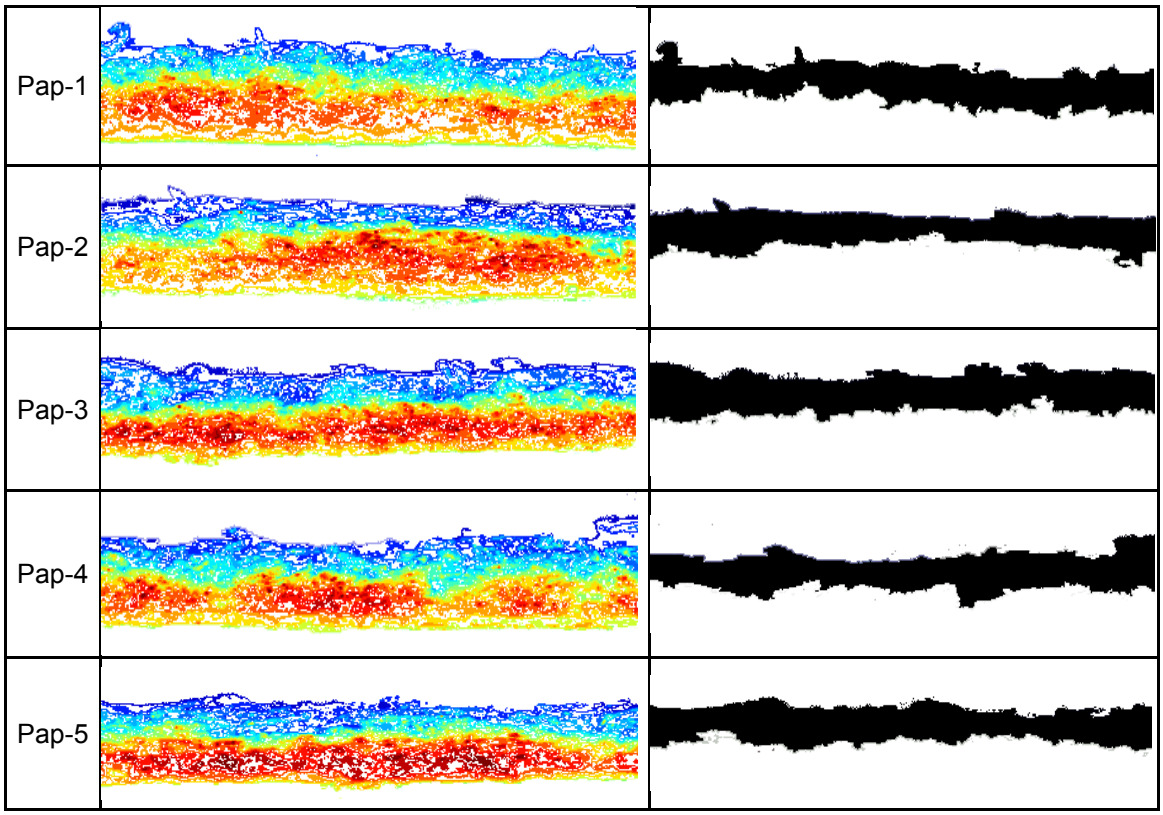

Fig. 5. Contours and ink layers for different paper types. The cold tones (from cyan to blue) in the contour map indicate ink penetration, whereas warm tones (from yellow to red) indicate the substrate paper.

Table. 3. Data of Average Depth of Ink Penetration and Variation

Handsheet	Average Depth (μ m)	Variance
Pap-1	68.62	178.25
Pap-2	59.68	247.40
Pap-3	63.06	127.65
Pap-4	57.68	308.92
Pap-5	43.25	180.37

Average Ink Permeability and Ink Distributions

Figure 6 presents the schematic diagram of the average ink permeability and ink distributions. The ink permeability in each column ($P(i)$), the average ink permeability (P), and the ink distributions in the paper interior (Q) were calculated using Eqs. 4, 5, and 6:

$$P(i) = \frac{y_1(x_i) - y_0(x_i)}{y_2(x_i) - y_0(x_i)} \times 100\% \quad (4)$$

$$P = \frac{\sum_1^n P(i)}{\mathrm{n}} \quad (5)$$

$$Q(j) = \frac{s \times N(j)}{S} \times 100\% \quad (6)$$

$$S = 5 \times n$$

$$s = \frac{1}{n} \times S$$

where i is the number of the column; i= [1, n]; and N(j) is the number of the s containing ink in a certain layer. j= 0, 5, …,100.

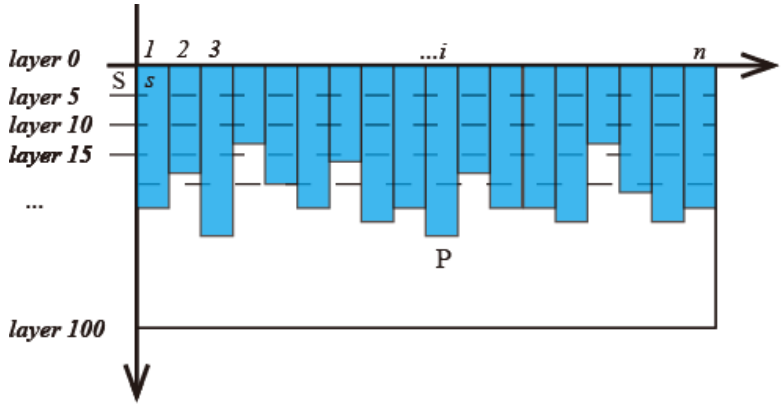

Fig. 6. The average ink permeability (P) in each column. Ink distributions (Q) in the paper interior were calculated by dividing the paper thickness along the Z-direction from top (paper surface) to bottom, into 100 average layers spaced at intervals of 5.

As is presented in Fig. 7, the average ink permeability of Pap-1 was 37.49%. Due to the sizing agent making the fibers' surface hydrophobic, Pap-2 showed the lowest average permeability of 34.43%; in contrast, when the filler was added to Pap-3, the filler made the paper structure looser and more porous, giving Pap-3 the highest ink permeability of the paper types, which was 44.07%.

The ink permeability of Pap-4 was 42.04%. Since the calendering made the structure of Pap-5 more compact, its permeability was slightly lower than that of Pap-4,

reaching 40.40%. Generally, the uncoated paper types, Pap-1 through Pap-5, exhibited deeper ink penetration depth and higher permeability than did the coated paper.

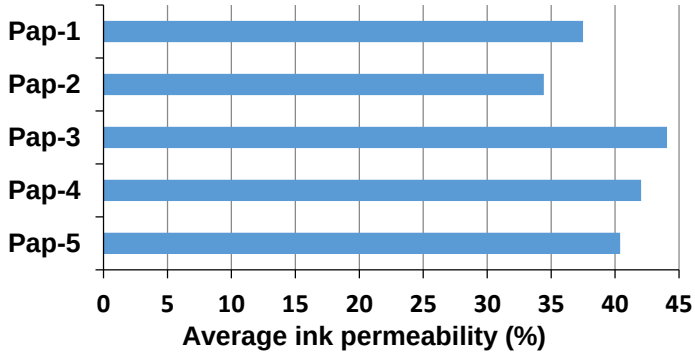

Fig. 7. The average permeability of different papers

As Fig. 8 depicts, the ink distributions of the different paper sheets all had a stable state at the paper surface layer. Then as the layer was increased, papers with different compositions showed various declining rates. At layer 15, the ink distributions of Pap-2 began to decrease ahead of Pap-1 and Pap-3, revealing that water-based ink only completely covered the top 15 layers of Pap-2 paper thickness. At layer 55, both ink distributions in Pap-1 and Pap-2 decreased to 0, showing that there were no more ink traces found deeper than 50 layers of the paper thickness. By comparison, the declining rate of Pap-2 was most dramatic, suggesting that "layer to layer" variation of Pap-2 was also largest. However, the ink distributions of Pap-3 did not decline until layer 30, ending at layer 65. Meanwhile, the curve of Pap-3 had a longer extending and slower rate of decline. All these indicate that ink droplets in the Pap-3 interior traveled a more unobstructed path and penetrated into a deeper position. The ink distributions of Pap-1 sandwiched between Pap-2 and Pap-3, allowing a comparison of how the different compositions affecting the ink distributions.

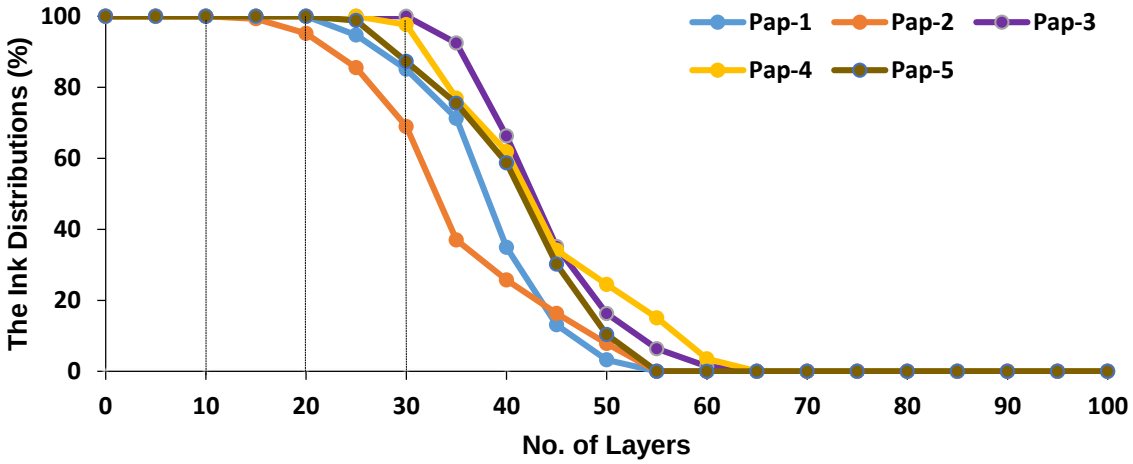

Fig. 8. The distributions of water-based ink in the paper interior

The curves of Pap-4 and Pap-5 present the ink distributions depending on the calendering process. Because of the more compact structure of Pap-5, the pigments were more likely to be concentrated near the surface. Thus, the ink distributions of Pap-5

emerged at layer 20, an earlier falling point. At layer 55, there were no more ink traces found in Pap-5, unlike the same layer in Pap-4 (approximately 15.06%). Moreover, the overall rate of decline was faster for Pap-5 than for Pap-4.

Effect on Printability of Uncoated Inkjet Paper

Color gamut and optical density

The color gamut value was obtained from the *a** and *b** values of the solid C, M, and Y together with the R, G, and B patches, and was calculated as the area of the (*a**, *b**) -hexagon. This definition of the color gamut represents a simplified top-view of the full 3-dimensional gamut volume in the CIE *L***a***b** color space obtained by considering the corresponding *L** values.

As depicted in Fig. 9, ink penetration did produce various color ranges and optical densities. Due to the sizing agent, the ink vehicle prevented pigment particles from penetrating into a deep position in Pap-2, which resulted in the concentration of pigment particles close to the paper surface. As a result, the color range and color density increased a little more than Pap-1. Water-based pigment ink in Pap-2 with fillings produced a poor print quality because of the unobstructed penetration in a porous structure.

The color range and optical density of Pap-4 improved quantitatively over Pap-2 and Pap-3, indicating that the presence of both the sizing agent and fillings was able to yield better print quality. Of the different sheets, Pap-5 achieved the most satisfactory outcome. Moreover, it could be concluded that the presence of a sizing agent (in Pap-2, Pap-4, and Pap-5) led to a wider color gamut and higher optical density in comparison to the paper sheets lacking the sizing agent (Pap-1, Pap-3). Furthermore, the color gamut and optical density of Pap-5 reached a new level because of the calendering.

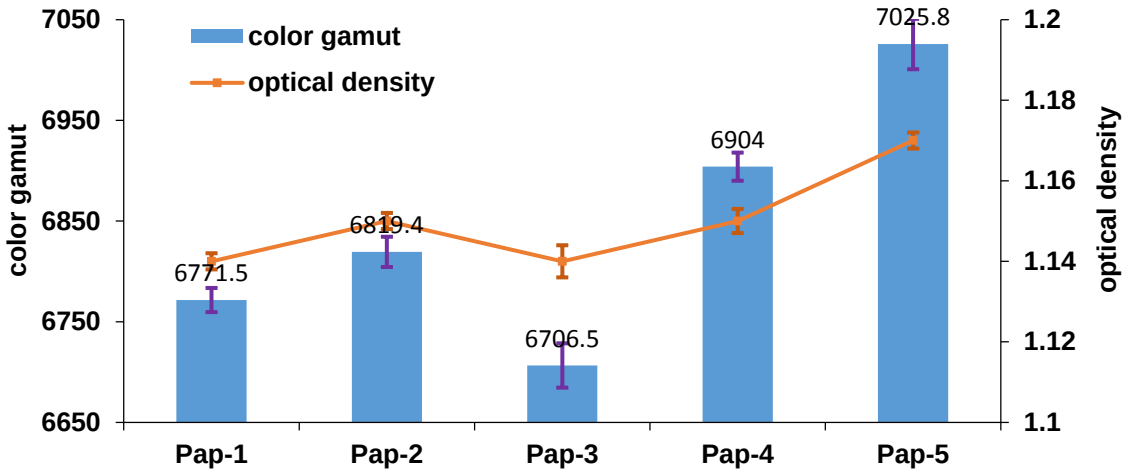

Fig. 9. Color gamut and optical solid density of yellow ink with different hand-sheets

Hues and saturation

Figure 10 shows a two-dimensional plane of *a** and *b** values of CMY and RGB of different dot area ratios from 0 to 100%. Ideally, if the curve is linear with the increasing dot area ratios, the paper will achieve a better consistency in color hue and a more stable color; on the other hand, the farther the curve extends from the coordinate origin, the higher color saturation can be expected for the paper. As can be seen, the ink penetration did affect the color hues and saturation. Figures 10 (1) and (2) depict the maximum saturation for

yellow. The curves of all hues at larger dot area ratios happened to an obvious twist except the yellow, revealing that may be negative to a dark color reproduction because of the changed hues.

Even so, Fig. 10 (1) shows that the saturation of Pap-2 was slightly higher than that of Pap-1 and Pap-3; Fig. 10 (2) also shows that the curve of Pap-5 extended farther than Pap-4, and the color saturation greatly increased. On the whole, the ink penetration produced different color arrays, color densities, hues, and color saturations depending on the paper sheet tested.

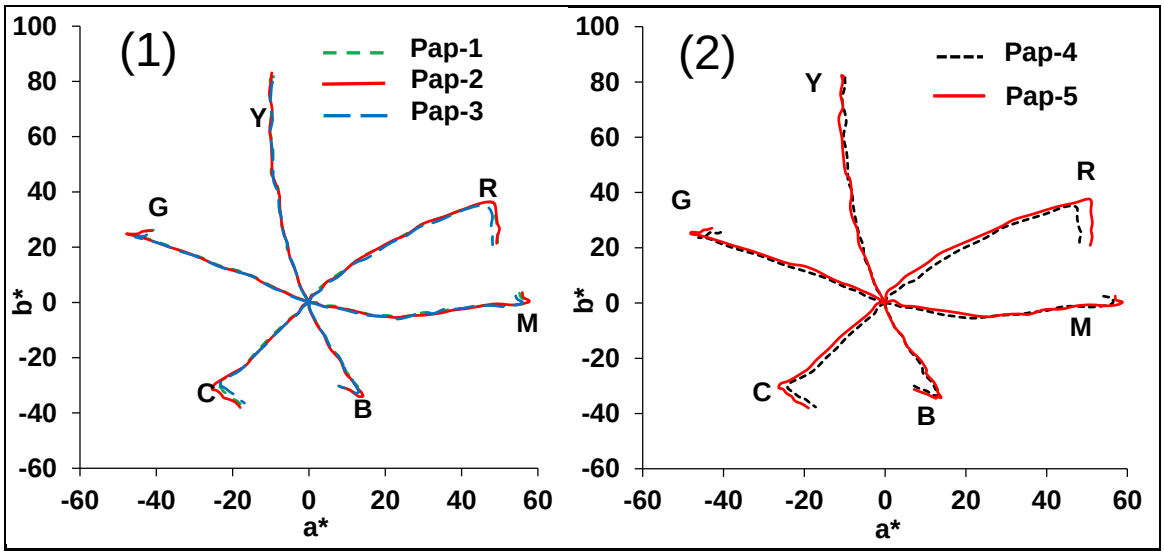

Fig. 10. Color hues and saturation of the different sheets with different compositions or process

Contact angle, SEM and pore distribution

The contact angle measurement is a very useful tool for estimating the properties of the paper surface (Moutinho *et al.* 2007). Figure 11 gives the contact angles and shapes of the deionized water droplets on the surface of the five types of uncoated sheets when the droplets were on the substrate for 1 s.

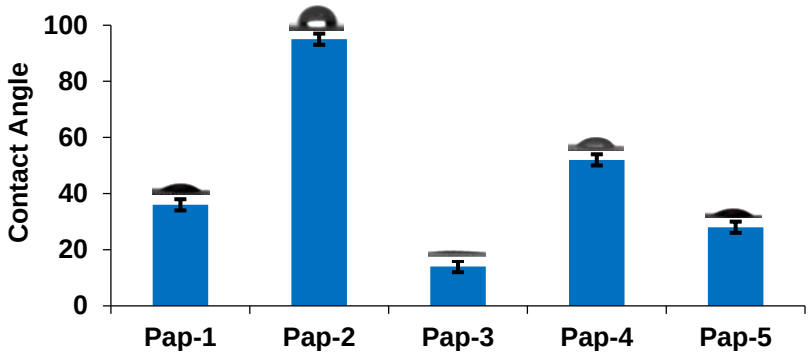

Fig. 11. Contact angles and shapes of deionized water droplets of the five papers

As can be seen, the contact angle of the water droplet onto Pap-1 was 32°. Since the internal AKD sizing imparted a hydrophobic nature to the fibers, the contact angle of the water droplet onto Pap-2 was the highest, at 95°. In contrast, the contact angle of the water droplet with Pap-3, with PCC, was the lowest, at 14°, which resulted in the rapid

absorption of the water droplet. Meanwhile, Pap-4, which combined AKD and PCC, exhibited a moderate contact angle of 52°. Moreover, the calendering in Pap-5 lowered the surface roughness and increased the compactness of the structure, which led to a lower contact angle than in Pap-4 (Schuman *et al.* 2003).

As Fig. 12 presents, Pap-1 contained only two kinds of fibers, and the hydrogen bond between the fibers gave Pap-1 a relatively uniform pore distribution, which facilitated an even ink distribution and a small variance of ink penetration (Table 3).

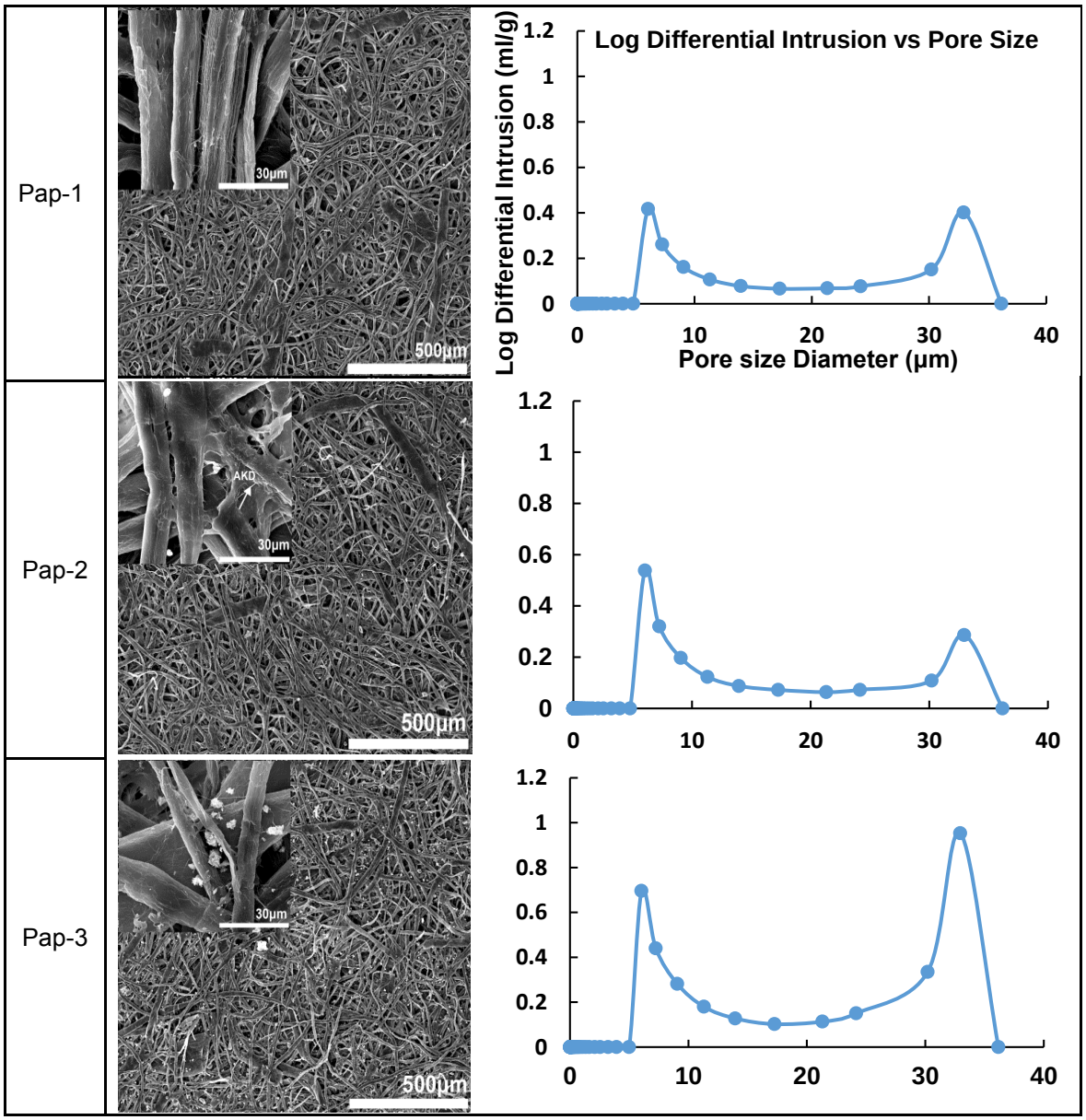

Fig. 12. SEM images of paper surfaces at different magnifications and pore distribution, displaying Pap-1, Pap-2, and Pap-3, respectively. Log differential intrusion (ml/g) means the volume of the mercury into sample of per gram. According to the density of mercury, it can be converted into the pore volume of the sample

Compared to Pap-1, the sizing agent did not change the paper porosity and pore distribution much. But the sizing agent in Pap-2 interacted with the fibers to form a hydrophobic layer on the fiber surface, which exhibited a certain resistance to the water-based ink penetration, thus increasing the contact angle of the ink droplets (Fig. 11) and decreasing the average ink penetration depth. However, as can be seen from the SEM image of Pap-2, the hydrophobic layer on the fiber surface had an inhomogeneous distribution, which may explain the volatile variance when water-based ink penetrated into Pap-2.

In Pap-3, the fillings were dispersed randomly throughout the paper interior, which weakened the mutual contacts and hydrogen bonding between the fibers, forming a large porosity and pore volume. Meanwhile, the large pores of Pap-3 large pores led to deeper penetration of ink pigments (Li and He 2011). In Pap-3, the water-based ink showed rapid absorption and penetration, allowing the ink to penetrate further, which reduced the residence time of ink on the paper surface and made the print dry faster. However, at the same time, the ink vehicle was able to penetrate deeper into the paper interior, which caused a decline in color density, color gamut, and saturation. It is worth mentioning that fillings can replace parts of fibers and in some cases reduce costs.

As can be seen in Figs. 9, 10, and 13, when both the sizing agent and fillings were added to Pap-4, the two materials may have mutual constraints. Water-based ink performed very differently when tested on Pap-2 versus on Pap-3, indicating that there was likely to be a mixture ratio balance between the two materials. The outcome of Pap-4 indicated that improvement in color range and optical density could be expected at a certain ratio of the sizing agent to filling.

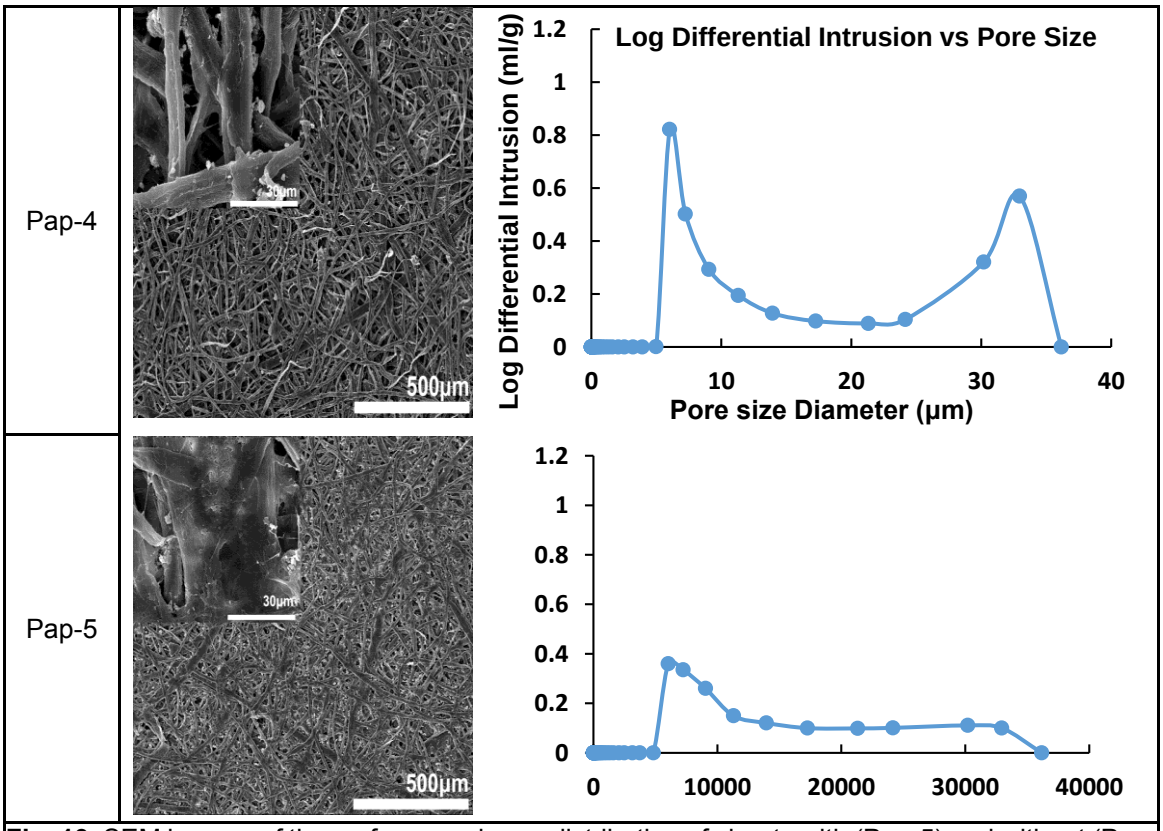

Fig. 13. SEM images of the surfaces and pore distribution of sheets with (Pap-5) and without (Pap-4) calendering

Figure 13 shows that the calendering not only improved the smoothness and glossiness of Pap-5, but also formed a very uniform pore distribution. The larger pores (> 30 μ m) were dramatically reduced. Besides, in terms of printability, color range, and color density, the paper sheet significantly improved (Fig. 9). In fact, the calendering substantially altered the paper surface and its internal porosity, forming a more compact structure, within which ink pigment particles were more likely to become concentrated. As a result, Pap-5 showed a better print quality.

CONCLUSIONS

1. A novel investigation on the penetration depth and permeability of water-based ink on uncoated inkjet paper was quantitatively conducted with image technology. The effect of differently composed or processed paper on ink distributions could be obtained.
2. The internal sizing agent produced a hydrophobic layer on the fiber surface, resulting in reduced water-based ink penetration and an inhomogeneous distribution. Filler particles in the paper interiors resulted in increased porosity and pore volume, leading to an increased ink penetration and deeper ink distribution. When combined with sizing, filler, and the calendering at a certain ratio, paper with certain combinations achieved a more compact structure and allowed the print quality to reach a new level.
3. The paper surface properties (hydrophobic) and paper internal structure (porosity and pore distribution) both had an effect on ink penetration. When tested on sheets of different parameters, ink penetration led to varying print qualities, including color gamut, optical density, color hues, and saturation. These results provided some insight into ink-paper interactions.

ACKNOWLEDGMENTS

The authors are grateful for the support of the National Natural Science Foundation of China, grant no. 31370583.

REFERENCES CITED

Bülow, K., Kristiansson, P., Schüler, B., Tullander, E., Östling, S., Elfman, M., Malmqvist, K., Pallon, J., and Shariff, A. (2002). "The penetration depth and lateral distribution of pigment related to the pigment grain size and the calendering of paper," *Nuclear Instruments and Methods in Physics Research Section B: Beam Interactions with Materials and Atoms* 189(1), 308-314. DOI: 10.1016/S0168-583X(01)01076-X.

Daniel, R. C., and Berg, J. C. (2006). "Spreading on and penetration into thin, permeable print media: Application to ink-jet printing," *Advances in Colloid and Interface Science* 123-126, 439-469. DOI:10.1016/j.cis.2006.05.012.

Emmel, P., and Hersch, R. D. (2002). "Modeling ink spreading for color prediction," *Journal of Imaging Science and Technology* 46(3), 237-246.

Heard, P., Preston, J., Parsons, D. J., and Allen, G. C. (2004). "Visualisation of the distribution of ink components in printed coated paper using focused ion beam techniques," *Colloids and Surfaces A: Physicochemical and Engineering Aspects* 244(1), 67-71. DOI:10.1016/j.colsurfa.2004.05.012.

Kishida, T., Kouichirou, A., Fukui, T., and Kanou, S. (2001). "Influence of coating pore structure and ink set property on ink dryback in sheet-fed offset printing," TAPPI Coating Conference and Trade Fair, San Diego, CA, United States.

Kubelka, P. (1948). "New contributions to the optics of intensely light-scattering materials. Part I," *JOSA* 38(5), 448-448. DOI:10.1364/JOSA.38.000448.

Kubelka, P., and Munk, F. (1931). "An article on optics of paint layers," *Z. Tech. Physical* 12(5), 593-595.

Le, H. P. (1998). "Progress and trends in ink-jet printing technology," *Journal of Imaging Science and Technology* 42(1), 49-62.

Li, Y., and He, B., H. (2011). "Characterization of ink pigment penetration and distribution related to surface topography of paper using confocal laser scanning microscopy," *BioResources* 6(3), 2690-2702. DOI: 10.15376/biores.6.3.2690-2702

Li, Y., and Miklavcic, S. J. (2005). "Revised Kubelka-Munk theory. III. A general theory of light propagation in scattering and absorptive media," *JOSA* A22(9), 1866-1873. DOI:10.1364/JOSAA.22.001866.

Li, Y., and Kruse, B. (2000). "Ink penetration and its effects on printing," *Proc. SPIE 3963, Color Imaging: Device-Independent Color, Color Hardcopy, and Graphic Arts V*, 365 (December 21, 1999). DOI: 10.1117/12.373417.

Li, Y., Fogden, A., Pauler, N., Sävborg, Ö., and Kruse, B. (2005). "A novel method for studying ink penetration of a print," *Nordic Pulp and Paper Research Journal* 20(4), 423-429. DOI:10.3183/NPPRJ-2005-20-04-p423-429.

Mattila, U., Tahkola, K., Nieminen, S., and Kleen, M. (2003). "Penetration and separation of coldset ink resin and oils in uncoated paper studied by chromatographic methods," *Nordic Pulp and Paper Research Journal* 18(4), 413-420. DOI: 10.3183/NPPRJ-2003-18-04-p413-420.

Moutinho, I. M. T., Ferreira, P. J. T., Figueiredo, M. L. (2007). "Impact of surface sizing on inkjet printing quality," *Industrial and Engineering Chemistry Research* 46(19), 6183-6188. DOI: 10.1021/ie070356k.

Ozaki, Y., Bousfield, D., and Shaler, S. (2005). "Three-dimensional characterization of ink vehicle penetration by laser scanning confocal microscopy," *Journal of Pulp and Paper Science* 31(1), 48-52.

Schuman, T., Wikström, M., and Rigdahl, M. (2003). "The effect of hot calendering of the substrate on the barrier properties of poly(vinyl alcohol)-coated papers," *Nordic Pulp and Paper Research Journal* 18(1), 81-89. DOI: 10.3183/NPPRJ-2003-18-01-p081-089.

Varjos, P., Kataja, K., Lipponen, M., and Leino, P. Q. (2004). "Absorption studies of coldset ink components into paper," 11th International Printing and Graphics Arts Conference, Vol. 1, Bordeaux Lac, France, Pairs.

Article submitted: June 18, 2015; Peer review completed: August 26, 2015; Revised version received and accepted: October 3, 2015; Published: October 26, 2015.
DOI: 10.15376/biores.10.4.8135-8147